J Mater Sci (2009) 44:3968–3974
DOI 10.1007/s10853-009-3541-5

Effect of the La_2O_3 sol–gel coating on the alumina scale adherence on a model Fe–20Cr–5Al alloy at 1100 °C

H. Buscail · C. T. Nguyen · R. Cueff · C. Issartel · F. Riffard · S. Perrier

Received: 29 January 2009 / Accepted: 2 May 2009 / Published online: 21 May 2009

Abstract The effect of lanthanum sol–gel coatings was studied in order to improve the alumina scale adherence during the model Fe–20Cr–5Al alloy oxidation, at 1100 °C, in air. Various sol–gel coating procedures were applied. Argon annealing of the lanthanum sol–gel coating was tested at temperatures ranging between 600 and 1000 °C. The coating crystallographic nature was characterized by X-ray diffraction (XRD) depending on the annealing temperature. The oxidation process has been examined at 1100 °C by in situ XRD on blank Fe–20Cr–5Al, sol–gel coated and argon-annealed specimens. This study shows that the coating argon annealing at 1000 °C leads to the preferential formation of $LaAlO_3$ instead of La_2O_3. This coating procedure leads to an alumina scale formation showing the best adherence under thermal cycling conditions at 1100 °C.

Introduction

Alumina-forming alloys, FeCrAl, containing 20% chromium and 5% aluminium are often used in electrical heating elements at high temperatures. The alumina scale generally insures a good oxidation protection under isothermal conditions. Nevertheless, under thermal cycling conditions scale spallation generally occurs [1–3]. The literature has shown that reactive elements, such as Ce, Y or La, can improve the protective character of the alumina scale and its adherence on the alloy. Most of the authors presented results about the effect of rare earth elements, introduced as alloying elements or by ion implantation on the alloy [4–6].

The aim of this study is to present another coating procedure, which consists in a lanthanum sol–gel coating deposited on the alloy surface. It focuses on the effect of lanthanum on the scale adherence on a model FeCrAl alumina-forming alloy oxidized at 1100 °C. The model FeCrAl alloy studied is free of impurities or minor elements. The effect of the lanthanum sol–gel coating was studied. It was compared with different argon annealing conditions at 600, 800 and 1000 °C prior to oxidation to examine the nature and efficiency of the coating. Thermal cycling tests were performed in order to compare the oxide scale adherence with the different surface treatments. Kinetic studies and in situ X-ray diffraction (XRD) will lead to explain the oxidation mechanism involved and the effect of the argon annealing on the alumina scale adherence.

Experimental details

The FeCrAl alloy used in this study is a high-purity alloy provided by Prof. J. Le Coze from l'Ecole des Mines de Saint-Etienne (France). The alloy composition is given in Table 1. The samples are 1-mm-thick disks of 14-mm-diameter. The blank specimens were polished on SiC paper up to the 600 polishing grade, then washed with ethanol and finally dried just before isothermal oxidation at 1100 °C or sol–gel coating. The 0.4 mol/L lanthanum hydroxide solution is obtained from the precipitation of lanthanum hydroxide in 0.27 mol 28% ammonia. After filtration the

H. Buscail (✉) · C. T. Nguyen · R. Cueff · C. Issartel · F. Riffard · S. Perrier
LVEEM, Laboratoire Vellave sur l'Elaboration et l'Etude des Matériaux, 8 rue J.B. Fabre, BP 219, 43006 Le Puy-en-Velay Cedex, France
e-mail: buscail@iut.u-clermont1.fr

Table 1 Composition of the model FeCrAl alloy (wt%)

FeCrAl	Fe	Cr	Al	C	S	O	N
wt%	Bal.	19.98	5.00	<0.001	<0.001	<0.001	<0.001

dissolution of the precipitate is obtained in the 69% nitric acid at 60 °C [7]. The lanthanum sol–gel coatings are carried out by dipping the specimens for 10 s in the solution. After drying for 10 min in a 50 °C air flux, the coating thickness is closed to 0.5 μm. After sol–gel coating, the argon annealing was performed in a quartz reaction tube. A heating ramp is applied at a rate of 5 °C/min until the 600, 800 or 1000 °C annealing temperature is reached. The temperature is maintained for 2 h. Then the specimen is cooled down at 5 °C/min to room temperature. In order to compare the various surface treatments, five kinds of specimens have been tested; they are listed in Table 2.

Kinetic results under isothermal conditions were recorded by means of a Setaram TG-DTA 92-1600 microthermobalance, for 100 h, at 1100 °C in air. The in situ characterization of the oxide scales was carried out in a high-temperature MRI chamber adapted on an X-ray Philips X' PERT MPD diffractometer (copper radiation, $\lambda k_\alpha = 0.154$ nm). The XRD conditions were 2Θ scan, step size of 0.05° ranging from 10 to 80°, 2.5 s counting time. Each in situ XRD pattern is obtained within 1 h in the 10–80° 2Θ range. The morphology of the external surface as well as the specimen cross sections were observed with secondary electrons using a scanning electron microscope (SEM) JEOL JSM-6400F. The analysis of the scale was performed with the LINK energy dispersive X-ray spectroscopy (EDS).

Thermal cycling was performed in static laboratory air at atmospheric pressure in a classical tubular furnace. Three samples were placed at the same time into an alumina crucible to estimate the reproducibility. The thermal cycle consists in a 20-h exposure at high temperature, followed by a duration of 4 h at room temperature after air quenching. The weight change of the samples was determined after each cycle on a balance with an accuracy of ±0.1 mg.

Table 2 Various surface treatments and corresponding specimen labels

Specimen surface treatment	Specimen label
Model FeCrAl (blank)	FeCrAl
FeCrAl lanthanum sol–gel coating without annealing	sg La
FeCrAl lanthanum sol–gel coating with argon annealing at 600 °C	sgLa.ann.600
FeCrAl lanthanum sol–gel coating with argon annealing at 800 °C	sgLa.ann.800
FeCrAl lanthanum sol–gel coating with argon annealing at 1000 °C	sgLa.ann.1000

Results

Isothermal oxidation at 1100 °C in air

The mass gain curves obtained after FeCrAl isothermal oxidation at 1100 °C are shown in Fig. 1. These curves allow us to compare the results obtained with all the specimens: FeCrAl, sg La, sgLa.ann.600, sgLa.ann.800 and sgLa.ann1000. In all cases the kinetic curves follow a parabolic behaviour. The parabolic rate constants, k_p, were calculated from the slope of the line obtained on a $\Delta m/S$ vs. $t^{1/2}$ plot [8]. The calculated k_p values are reported in Table 3. It appears that these values are higher for the argon-annealed specimens. The FeCrAl and "sg La" specimens show similar k_p values.

Cyclic oxidation

The specimen mass change versus the number of cycles is shown in Fig. 2. It shows that the oxide scale is not always adherent to the substrate. FeCrAl specimens lead to a scale spallation after only two cycles. The lanthanum sol–gel coating (sg La) has a slight beneficial effect on the oxide

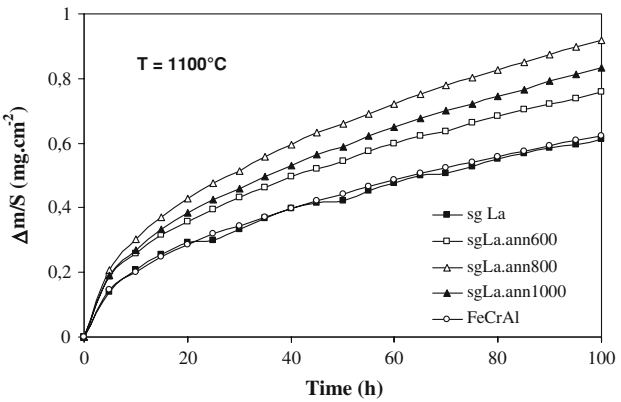

Fig. 1 Mass gain curve obtained after isothermal FeCrAl oxidation at 1100 °C

Table 3 Parabolic rate constants obtained after oxidation at 1100 °C, 100 h, in air

Specimen surface state	k_p ($g^2/cm^4/s$)
FeCrAl	1.13×10^{-12}
sg La	1.07×10^{-12}
sgLa.ann.600	2.06×10^{-12}
sgLa.ann.800	2.33×10^{-12}
sgLa.ann.1000	1.98×10^{-12}

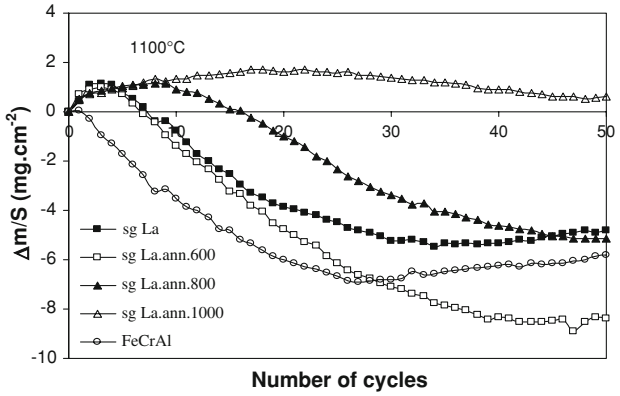

Fig. 2 Specimens mass change versus the number of cycles at 1100 °C (20–4 h cycles)

scale adherence compared with blank specimens. The best adherence is observed when the specimen argon annealing has been performed at 1000 °C. In this case, very limited spallation occurred during the cycling test.

XRD analysis

In situ X-ray patterns obtained on the FeCrAl specimen at 1100 °C are shown in Fig. 3. The oxide scale is only composed of α-alumina (JCPDS 46-1212). No transition alumina is detected during the initial stage oxidation. α-Alumina is detected from the first hour oxidation and grows continuously during the 30 h oxidation without showing any phase transformation. In situ XRD patterns obtained on the "sg La" specimen at 1100 °C are shown in Fig. 4. No lanthanum-containing oxides were detected before oxidation at 1100 °C. This is due to the fact that the sol–gel coating does not lead to sufficiently crystallized species to be detected by XRD. After heating up to 1100 °C, α-alumina appears very quickly and grows with time. During the first hour oxidation, if alumina is the major phase present on the alloy, XRD patterns also show the presence of three lanthanum-containing oxides: La_2O_3 (JCPDS 05-0602), $LaAlO_3$ (JCPDS 31-0022) and $LaAl_{11}O_{18}$ (JCPDS 33-0699) which appear simultaneously. The La_2O_3 peaks intensity decreases with time and becomes undetectable after 2 h oxidation. It appears that La_2O_3 is transformed into $LaAlO_3$ and $LaAl_{11}O_{18}$ with time. In situ X-ray patterns obtained on the "sgLa.ann.600" specimen oxidized at 1100 °C are shown in Fig. 5. Before oxidation, we have noticed the presence of La_2O_3 and $LaAl_{11}O_{18}$ on the surface. At 1100 °C, the La_2O_3 peaks completely disappear after the first hour of oxidation. $LaAl_{11}O_{18}$ peaks also become undetectable after 10 h, whereas the $LaAlO_3$ peaks grow during the first 10 h. In situ X-ray patterns obtained on the "sgLa.ann.800" specimen oxidized at 1100 °C are shown in Fig. 6. On the initial surface, the

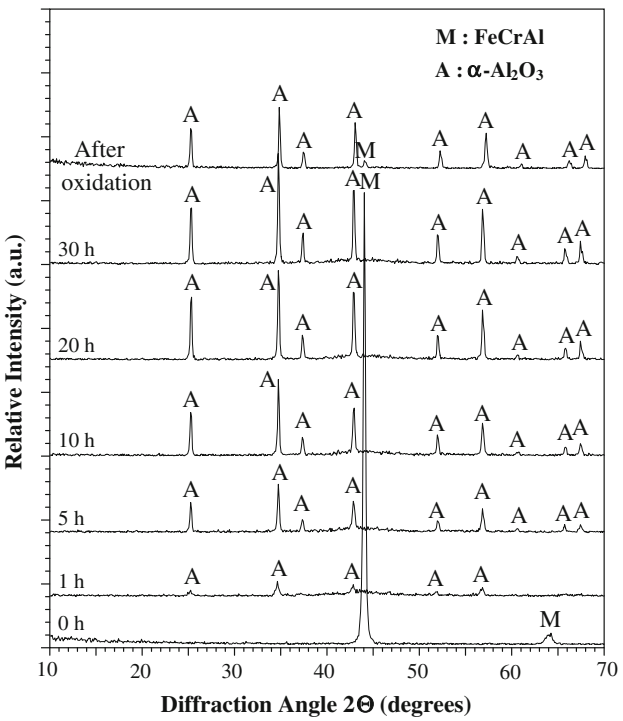

Fig. 3 In situ XRD patterns obtained on the FeCrAl specimen, at 1100 °C

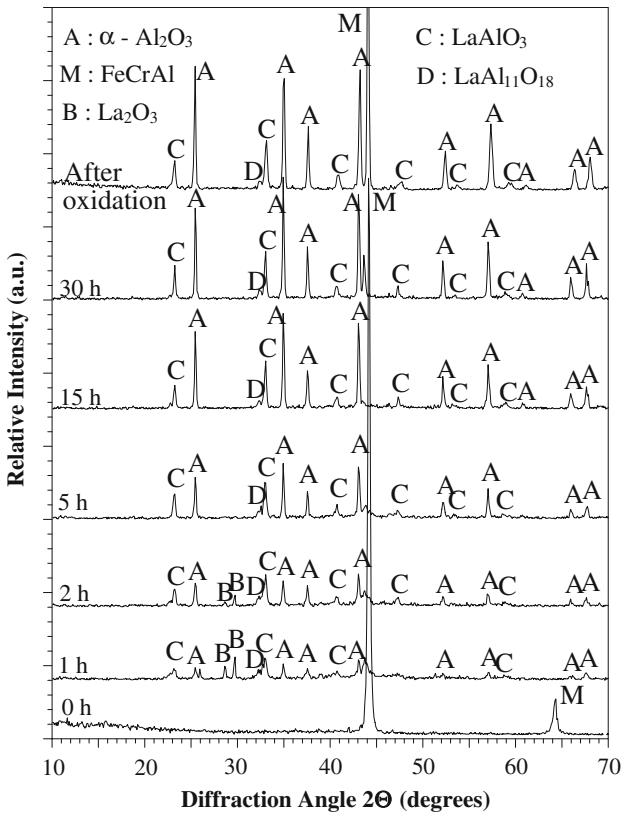

Fig. 4 In situ XRD patterns obtained on the "sg La specimen" at 1100 °C

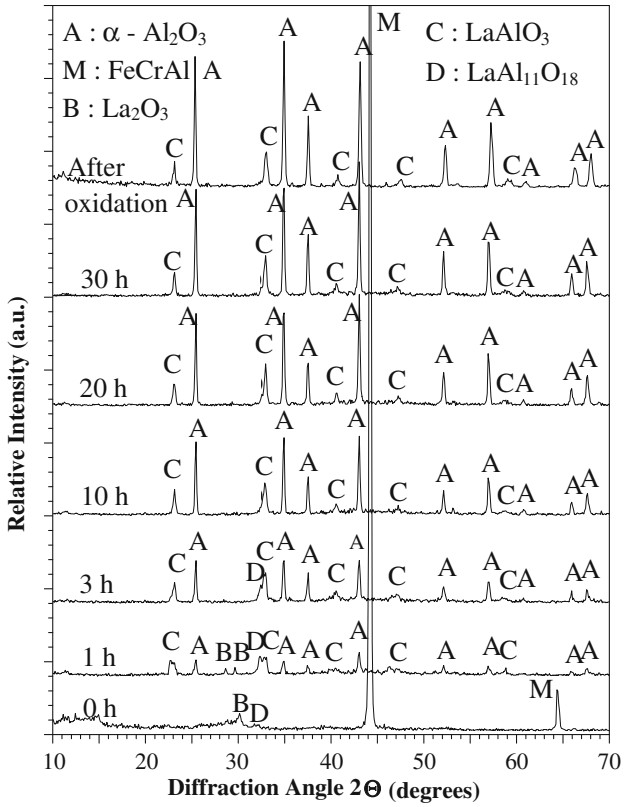

Fig. 5 In situ XRD patterns obtained on the "sgLa.ann.600" specimen at 1100 °C

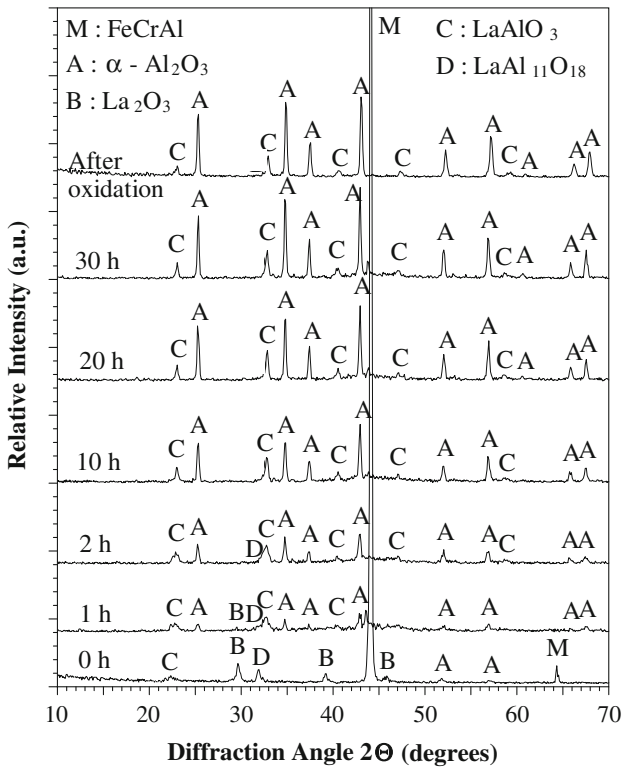

Fig. 6 In situ XRD patterns obtained on the "sgLa.ann.800" specimen, at 1100 °C

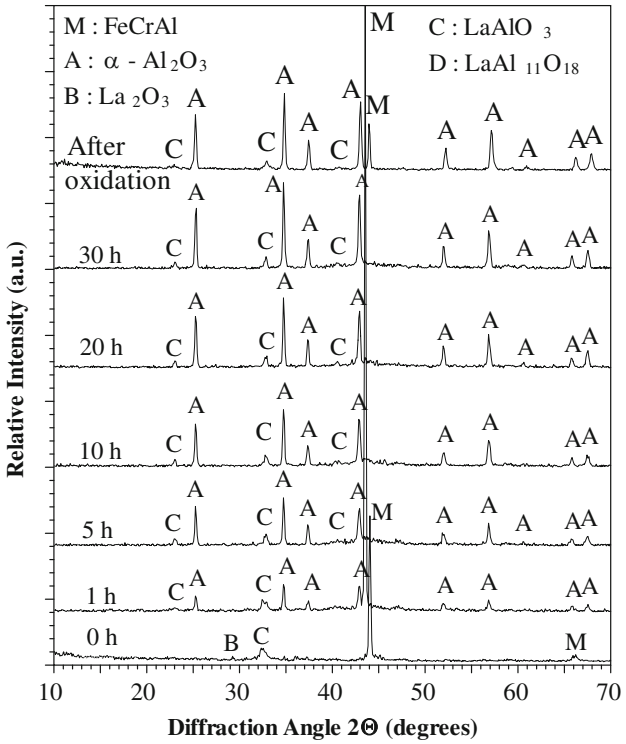

Fig. 7 In situ XRD patterns obtained on the "sgLa.ann.1000" specimen, at 1100 °C

lanthanum-containing oxide La_2O_3 is present on the surface with $LaAl_{11}O_{18}$. During the oxidation at 1100 °C, the La_2O_3 and $LaAl_{11}O_{18}$ peaks completely disappear after the second hour of oxidation, whereas the $LaAlO_3$ peaks grow with time. In situ X-ray patterns obtained on "sgLa.ann.1000" specimen at 1100 °C are shown in Fig. 7. On the initial surface, $LaAlO_3$ appears as the major lanthanum-containing phase on the surface. The small La_2O_3 peaks disappear during the first hour oxidation. All along the 30 h oxidation test the $LaAl_{11}O_{18}$ has never been detected on the surface of the "sgLa.ann.1000" specimen and after cooling to room temperature.

After 150 h oxidation, XRD patterns show that on all kinds of lanthanum sol–gel coated specimens, $LaAl_{11}O_{18}$ can be detected on the surface after oxidation (Fig. 8). This shows that if after 30 h oxidation $LaAl_{11}O_{18}$ is not detected at room temperature it is found after long-term testing.

Scale cross section of the sgLa.re1000 specimen oxidized at 1100 °C

SEM examinations were carried out on the sgLa.re1000 specimen cross section (Fig. 9) in order to estimate the subscale thickness and to identify the elements incorporated in the oxide scale. After 150 h oxidation at 1100 °C, the adherent scale is 4 ± 0.5 μm thick. EDS analyses are shown in Fig. 10. The scale bulk is composed of alumina

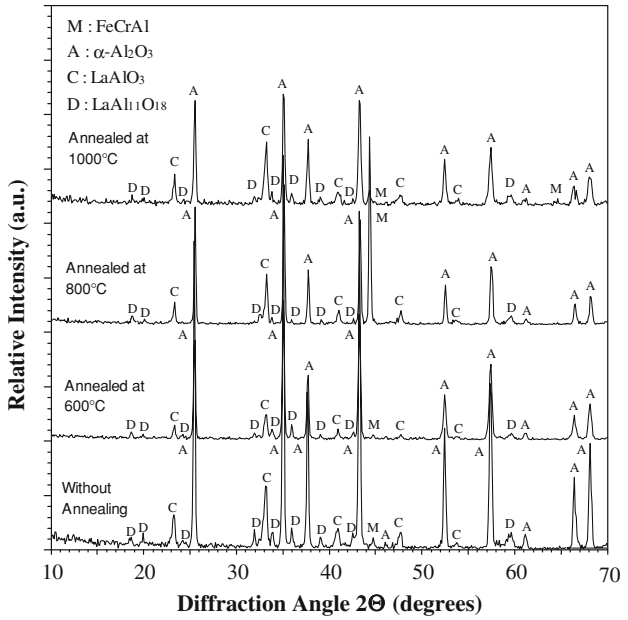

Fig. 8 XRD patterns obtained on coated specimens oxidized 150 h, at 1100 °C

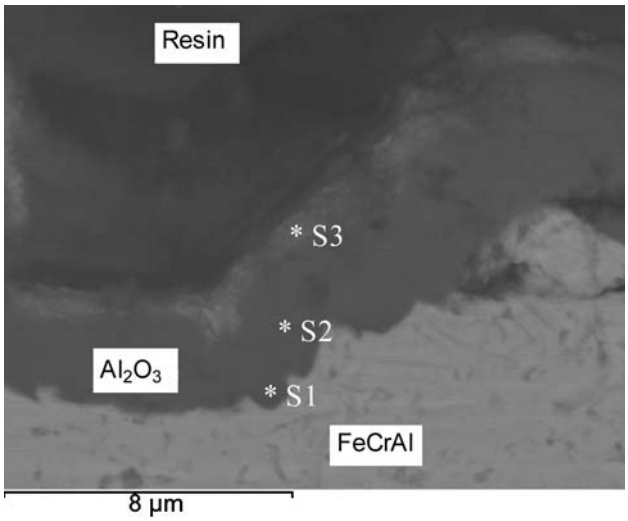

Fig. 9 Scale cross section observed on the sgLa.re1000 specimen oxidized at 1100 °C, in air for 150 h

(spectra 1 and 2). It appears that lanthanum is mainly located close to the air/oxide interface (spectrum 3).

Discussion

According to the isothermal kinetic results shown in Fig. 1, it is shown that argon annealing of the lanthanum sol–gel coating always leads to a slight increase in the mass gain. This phenomenon is generally observed with lanthanum-

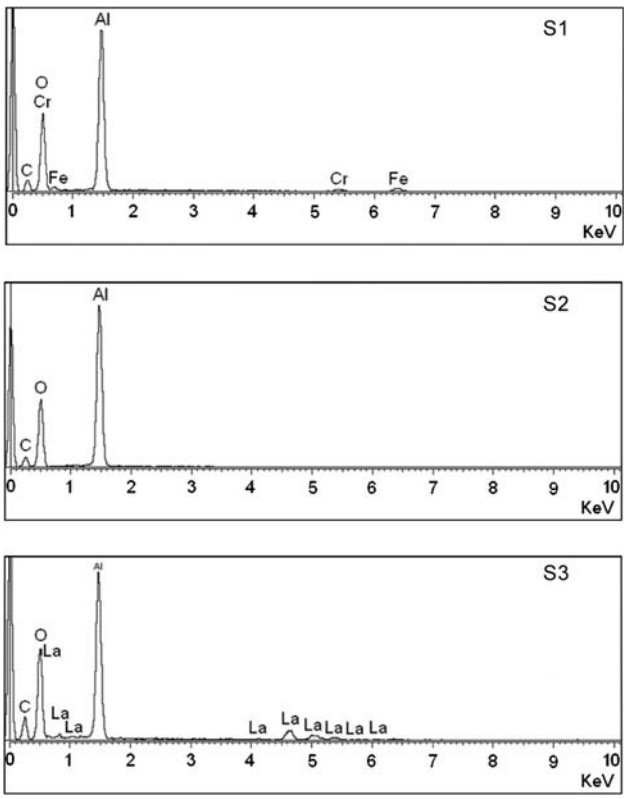

Fig. 10 EDS spectra obtained on the cross section of the sgLa.re1000 specimen oxidized at 1100 °C, in air, for 150 h

coated specimens due to the oxygen defective nature of the lanthanum-containing oxides [9]. Nevertheless, the protective character of the scale is maintained as long as the parabolic behaviour is followed and the scale acts as a diffusion barrier. Thermal cycling tests allow us to compare the scale adherence depending upon the FeCrAl specimen surface treatment. Figure 2 shows that the lanthanum sol–gel-coated specimens show a better α-Al_2O_3 scale adherence during the first cycles.

A drastic improvement of the α-alumina scale adherence is observed when the argon annealing is performed at 1000 °C. Thermodynamic assessments on the system La_2O_3–Al_2O_3 show that the two mixed oxide which can be formed are $LaAlO_3$ and $LaAl_{11}O_{18}$ [10]. In situ XRD results (Figs. 3–7) show that during the first 2 h of the oxidation test, the La_2O_3 peaks intensity decreases rapidly and the $LaAlO_3$ peaks' growth is observed. It means that a complete transformation of La_2O_3 into $LaAlO_3$ occurs according to reaction 1 [11, 12]:

$$La_2O_3 + Al_2O_3 \rightarrow 2LaAlO_3 \quad (1)$$

Moreover, in situ XRD and XRD patterns obtained after 150 h oxidation tests (Fig. 8) indicate that $LaAl_{11}O_{18}$ is the main lanthanum-containing phase observed after long-term

testing. This means that $LaAlO_3$ is progressively transformed into $LaAl_{11}O_{18}$ all along the oxidation process according to Eq. 2 [11, 12]:

$$LaAlO_3 + 5Al_2O_3 \rightarrow LaAl_{11}O_{18} \quad (2)$$

Ropp and Carroll [13] proposed that the La_2O_3 transformation into $LaAlO_3$ is a quick phenomenon, whereas the $LaAlO_3$ to $LaAl_{11}O_{18}$ transformation is a slower process. It is in accordance with our results obtained in situ and after 150 h oxidation. It then appears that reaction 2 has occurred after long-term testing. Key and Crist [14] have proposed that the La_2O_3–Al_2O_3 oxide mixture can provide two phases: a perovskite type oxide $LaAlO_3$ and a $LaAl_{11}O_{18}$ phase. Other authors have proposed that various factors influence the preferential formation of $LaAlO_3$ and/or $LaAl_{11}O_{18}$ from the La_2O_3–Al_2O_3 mixture. It depends on the La_2O_3/Al_2O_3 ratio [15], the reaction duration [12], the temperature [14], the oxygen pressure [12] and the preparation mode of the oxide precursors [13]. According to our results, it appears that the prevalent formation of each lanthanum-containing oxide is governed by the temperature, the oxidation duration and the ratio between La_2O_3 and Al_2O_3 on the specimen surface. Figure 4 shows that on the "sg La" specimen oxidized at 1100 °C, the oxides La_2O_3, $LaAl_{11}O_{18}$, $LaAlO_3$ and Al_2O_3 initially grow at the same time. Alumina is quickly formed due to the high oxygen pressure in air. Then, the alumina proportion in the oxide scale is high enough to lead to the $LaAl_{11}O_{18}$ formation from the beginning of the oxidation test.

When we consider the argon-annealed specimens at 600 and 800 °C, La_2O_3, $LaAl_{11}O_{18}$ and Al_2O_3 are formed under the low-oxygen residual pressure present in argon (around 10 ppm). Alumina nucleates on the specimen surface and La_2O_3 and $LaAl_{11}O_{18}$ are formed by crystallization of the initial sol–gel coating and reaction with alumina. Then, we have observed that the argon annealing temperature has a great influence on the coating composition (see the 0 h patterns in Figs. 5–7). The 1000 °C argon annealing temperature promotes the formation of $LaAlO_3$ due to the quick reaction 1 between La_2O_3 and Al_2O_3, which is thermally activated [11, 12]. At low argon annealing temperatures (600 and 800 °C), our results show that the La_2O_3 is not completely transformed and remains presented on the surface after annealing. The lowest annealing temperatures are not favourable to the $LaAlO_3$ formation because the reaction 1 rate is not high enough.

After isothermal oxidation, our kinetic results indicate that the highest parabolic rate constants are registered on lanthanum-coated annealed specimens. XRD results show that the $LaAl_{11}O_{18}$ formation is detected after long-term testing. These results are in accordance to what was proposed by Nair et al. [15] who indicate that the $LaAl_{11}O_{18}$ formation in the La_2O_3–Al_2O_3 mixture induces the oxide grain size growth and scale porosity and an increase in the oxidation rate. According to Hou et al. [9], lanthanum on the initial surface promotes the alumina growth on the surface and a higher mass gain in air, but it also favours the scale spallation. Reactive element oxides are also known to be oxygen defective structures. The higher mass gain observed on lanthanum-coated specimens can be due to a favoured oxygen transport in these oxide particles during the initial oxide growth mechanism on coated substrates [9]. Our results also show that increasing the argon annealing temperature reduces the initial amount of La_2O_3 on the substrate and improves the scale adherence. Nevertheless, our XRD results show that long-term oxidation tests always lead to the continuous increase in the Al_2O_3 amount in the scale. With time, such an alumina amount increase favours the $LaAlO_3$ transformation into $LaAl_{11}O_{18}$ mixed oxide.

Conclusion

In this study, thermal cycling tests indicate that the temperature of argon annealing of the lanthanum-containing sol–gel coating greatly improves the alumina scale adherence. XRD was performed in order to identify the coating crystallographic nature according to the argon annealing temperature ranging between 600 and 1000 °C. In order to follow the oxidation process at 1100 °C, in situ XRD was performed on blank Fe–20Cr–5Al, sol–gel-coated and argon-annealed specimens. Our results show that increasing the argon annealing temperature on lanthanum sol–gel-coated specimens up to 1000 °C leads to the preferential formation of $LaAlO_3$ instead of La_2O_3. The better alumina scale adherence under thermal cycling conditions is attributed to the presence of $LaAlO_3$ on the initial specimen surface before oxidation at 1100 °C. With time, $LaAlO_3$ is progressively transformed into $LaAl_{11}O_{18}$ after long-term oxidation.

References

1. Cueff R, Nguyen CT, Buscail H, Caudron E, Issartel C, Riffard F (2008) Mater Sci Forum 595–598:933
2. Chevalier S, Tankeu APD, Buscail H, Issartel C, Borchardt G, Larpin JP (2004) Mater Corros 55:610
3. Cueff R, Buscail H, Caudron E, Riffard F, Issartel C, El Messki S (2004) Appl Surf Sci 229:233
4. Golightly FA, Stott FH, Wood GC (1976) Oxid Met 10:163
5. Quadakkers WJ, Jedlinski J, Schmidt K, Krasovec M, Borchardt G, Nickel H (1991) Appl Surf Sci 47:261
6. Przybylski K, Garratt-Reed AJ, Pint BA, Katz EP, Yurek GJ (1987) J Electrochem Soc 134:3207
7. Czerwinski F, Szpunar JA (1997) J Sol-Gel Sci Technol 9:103

8. Pieraggi B (1987) Oxid Met 27:177
9. Hou PY, Shui ZR, Chuang GY, Stringer J (1992) J Electrochem Soc 139:1119
10. Fabrichnaya O, Zinkevich M, Aldinger F (2006) Int J Mater Res 97:1495
11. Barrera-Solano C, Esquivias L, Messing GL (1999) J Am Ceram Soc 82:1318
12. Zhang Q, Saito F (2000) J Am Ceram Soc 83:439
13. Ropp RC, Carroll B (1980) J Am Ceram Soc 63:416
14. Key TS, Crist B Jr (2005) J Am Ceram Soc 88:191
15. Nair J, Nair P, Mizukami F, Van Ommen JG, Doesburg GBM, Ross JRH, Burggraaf AJ (2000) J Am Ceram Soc 83:1942